Available online at www.sciencedirect.com
ScienceDirect
Journal of the European Ceramic Society 26 (2006) 3745–3752
www.elsevier.com/locate/jeurceramsoc

Growth and morphology of ZnO nanorods prepared from $Zn(NO_3)_2$/NaOH solutions

Juan Zhao, Zheng-Guo Jin *, Xiao-Xin Liu, Zhi-Feng Liu

Key Laboratory For Advanced Ceramics and Machining Technology of Ministry of Education, Tianjin University, Tianjin 300072, China

Received 9 September 2005; received in revised form 2 January 2006; accepted 14 January 2006
Available online 28 February 2006

Abstract

ZnO nanorods on ZnO-coated seed surfaces were fabricated by a solution chemical method using supersaturated $Zn(NO_3)_2$/NaOH solution. The seed surfaces were coated on glass substrates by sol–gel processing and PEG addition. The mechanism of crystal growth and the factors affecting the rod growth were elucidated. The morphology and structure of both the seed surface and successive nanorods were analyzed by using SEM, XRD, TEM and SAED. Nucleation on the ZnO seed surface is crucial for rod growth since rods can only be observed on ZnO-coated substrates. Supersaturation is also required for rod growth and the Zn^{2+} ion and NaOH concentrations must be varied synchronously to maintain the high level of supersaturation. The average diameter and length of the ZnO nanorods increase to different degree with increasing precursor concentration. The dependence of rod growth on temperature shows that the maximum rod growth rate at any given concentration of Zn^{2+} occurs at a specific temperature, and the optimal temperature increases with Zn^{2+} ion concentration. Densely thick nanorods oriented perpendicularly to the substrate can be obtained by controlling the seed surface with PEG assistance.

Keyword: ZnO nanorod

1. Introduction

One-dimensional semiconductor nanostructures have been extensively studied for their potential applications in manufacturing electronic and optoelectronic devices.[1] ZnO has a large direct band gap (3.37 eV), excellent chemical and thermal stability, and the electrical properties of a II–VI semiconductor possessing large exciton binding energy (60 meV). It has been recognized as one of the promising materials in a broad range of high-technology applications, e.g., surface acoustic wave filters,[2] photoniccrystals,[3] light-emitting diodes,[4] photodetectors,[5] optical modulator waveguides,[6] varistors,[7] gas sensors,[8] and solar cells.[9] The recent demonstration of room-temperature ultraviolet lasing from well-oriented ZnO nanowire or nanorod arrays (nanoarrays) has further stimulated substantial efforts to develop methodologies for the synthesis of one-dimensional ZnO nanostructures to be used for constructing electronic and optoelectronic devices.[10] Various chemical, electrochemical, and physical deposition techniques have been employed to create oriented arrays of ZnO NRs and nanowires, such as catalytic growth via the vapor–liquid–solid epitaxial (VLSE) mechanisms,[11] metalorganic chemical vapor deposition,[12] pulsed laser deposition,[13] and templating with anodic alumina membranes.[14] However, complex procedures, sophisticated equipment, or rigid experimental conditions are involved in these methods. In addition to these methods, a solution chemical route has become a promising option for large-scale production of the 1D nano-/microscale materials due to its simple, fast, and less expensive virtues. Izaki and co-workers prepared ZnO films by chemical reaction with dimethylamineborane (DMAB).[15,16] Highly oriented crystalline films were grown directly on a substrate in aqueous solutions containing urea as a chelating agent.[17] Thin films consisting of well-aligned ZnO microrods were formed by the thermal decomposition of an amino complex formed with Zn^{2+} and methenamine.[18,19]

We report here a new solution method for ZnO rod deposition that employ an aqueous solution containing NaOH and $Zn(NO_3)_2$ and substrates coated with ZnO as seeds through sol–gel processing. This method does not require the use of complexing agents and can produce micrometer-thick films in

* Corresponding author. Tel.: 86 22 27890266; fax: 86 22 27404724.
E-mail address: zhgjin@tju.edu.cn (Z.-G. Jin).

0955-2219/$ – see front matter © 2006 Elsevier Ltd. All rights reserved.
doi:10.1016/j.jeurceramsoc.2006.01.006

comparatively short times. Moreover, the strongly basic conditions lead to a more fixed and reproducible surface condition than the almost pH-neutral conditions of some other techniques. Meanwhile, due to the fact that the texture of the seed surface has great influence on the morphology and the alignment ordering of the ZnO nanorod arrays, we add PEG in the ZnO seed sol as surfactant to control the orientation and dimension of the seed grains and thus to improve the morphology, growth density and diameter of the grown nanorods. In this paper, the crystal growth mechanism was discussed and the supersaturation curves were supplemented using experimental data. Furthermore, the influence of parameters such as the precursor concentration, growth temperature, deposition time and the adding of PEG in the seed sol on rod growth was investigated.

2. Experimental procedure

2.1. Preparation of seed-coated substrates

$Zn(CH_3COO)_2{\cdot}2H_2O$ (0.75 mol/l) was first dissolved in a 2-methoxyethanol-monoethanolamine solution (0.75 mol/l) at room temperature. As for the experiments studying the effect of PEG, 0 g/50 ml, 1 g/50 ml, 2 g/50 ml and 4 g/50 ml of PEG were added in the mixture as well. The resultant solution was stirred at 60 °C for 30 min to yield a clear and homogeneous solution, which served as seed coating sol. Then a clean indium tin oxide (ITO, 10 Ω/□) glass substrate was dipped into the sol, withdrawn at 3.5 cm/min and dried in the air. Finally, the as-coated substrate was heated in an electrical furnace at 300 °C for 10 min, and the substrate with PEG was heated additionally at 500 °C for 1 h to remove the PEG thoroughly.

2.2. Measurement of supersaturation curves

The points on the supersaturation curves were determined by adding HNO_3 aqueous solution to lower the pH value of the clear $Zn(NO_3)_2$/NaOH solution under 30 °C and 90 °C. NaOH was first added to the $Zn(NO_3)_2$ solution with a certain concentration (10^{-4} M to 0.5 M) to produce a clear solution, then HNO_3 solution of pH 0.2 was used to titrate this solution until the solution just become turbid. The volume of consumed HNO_3 was recorded to compute the final Zn^{2+} concentration, and the pH was measured as well.

2.3. Growth of ZnO nanorods

The ZnO-coated substrates were rinsed with deionized water, and then suspended in aqueous solutions of $Zn(NO_3)_2$/NaOH with different ion concentrations, growth temperature varying from 30 °C to 90 °C and deposition time from 1.5 h to 12 h. The resultant samples were rinsed with deionized water and dried in air.

2.4. Characterization

The morphology of the ZnO nanorods was observed by field-emission scanning electron microscopy (FESEM, JEOL JSM6700 operated at 5 or 10 keV) and transmission electron microscopy (TEM, JEOL 100CX-II). The crystal structure of the seed surface and resultant nanorods was analyzed using XRD (Rigaku 2500) with Cu KR radiation at 40 kV/150 mA and HRTEM (JEOL JEM-2010).

3. Results and discussion

3.1. Physical mechanism of nanorod growth

Two processes are required for crystallization in a supersaturated solution: nucleation and crystal growth. The interface energy between ZnO/substrate is usually smaller than that of ZnO/solution. As a result, the nuclei tend to form on the substrate (heteronucleation) at a lower saturation ratio than in the solution (homogeneous nucleation). The interfacial tension between solution species and a crystal nucleation site depends on the degree of structural fit, the same crystal type having the best fit and lowest energy barrier.[20] Therefore, pre-coating the substrates with seeds of ZnO, the same material as the nanocrystals being grown, is an effective way to grow nanorods and to control their morphology, texture and even orientation. Although Vayssieres reported the growth of ZnO nanorods on unmodified substrates from solution of $Zn(NO_3)_2$ and methenamine, no rods of ZnO were observed on bare glass or ITO slides in our experiments, which indicates that the ZnO-seed particles play a crucial role in ZnO nanorod growth processes for the $Zn(NO_3)_2$/NaOH system. Meanwhile, on the ZnO-coated substrates, no matter glass or ITO slides, ZnO nanorods grew readily.

Fig. 1 shows a phase stability diagram for solid ZnO in which the solid line is the theoretical thermodynamic equilibrium curve between $Zn(OH)_4^{2-}$ and ZnO at 25 °C calculated on the basis of the thermodynamic data provided by reference,[21] and the dashed lines is the measured supersaturation curves for ZnO at 30 °C and 90 °C obtained from experiment. It can be seen that the supersaturation curve for 30 °C lies to the left of that for 90 °C, indicating that the solution is more stable at 30 °C than at 90 °C.

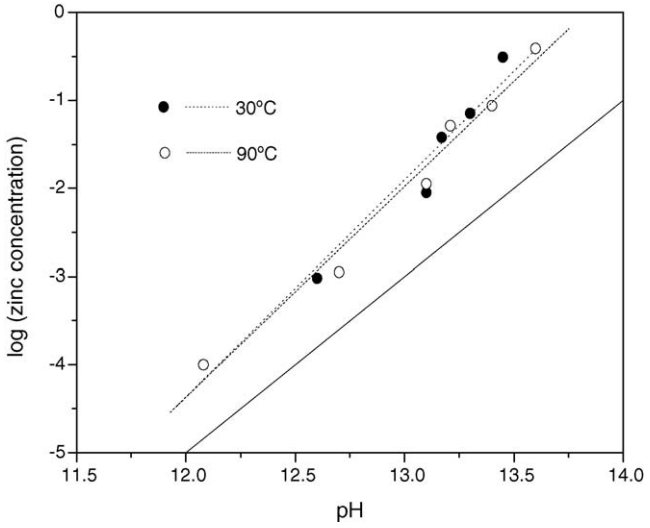

Fig. 1. Phase stability diagram for solid ZnO.

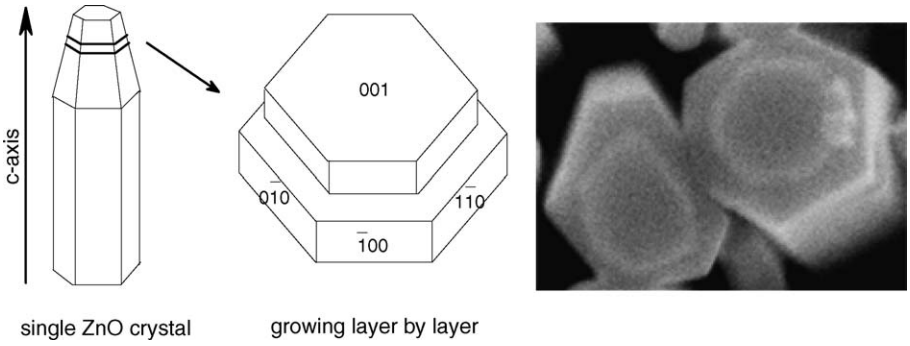

Fig. 2. Model corresponding SEM photograph of hexagonal ZnO single crystal.

It is known that supersaturation is the key driving force for crystal growth. In this case, the small metastable region between the two kinds of lines was suitable to produce ZnO nanorods without precipitation of other zinc species. More precisely, the amount of NaOH can only vary over a small range for a fixed Zn^{2+} concentration. When it was too high, the ZnO-coated substrate was etched away; if too low, ZnO and zinc hydroxide species precipitated out of solution. For ZnO rod growth, the following equation, where $n = 2$ or 4, was suspected to happen in solution[21]:

$$[Zn(OH)_n]^{2-n} + [Zn(OH)_n]^{2-n} \rightarrow [Zn_2O(OH)_{2n-2}]^{4-2n} + H_2O$$

The crystal structure of ZnO was first constructed by this dehydration between OH^- on the surface of the growing crystals and the OH^- ligands of the hydroxyl complexes. Fig. 2 is the model and corresponding SEM photograph of hexagonal ZnO single crystal showing its growth layer by layer along *c*-axis.

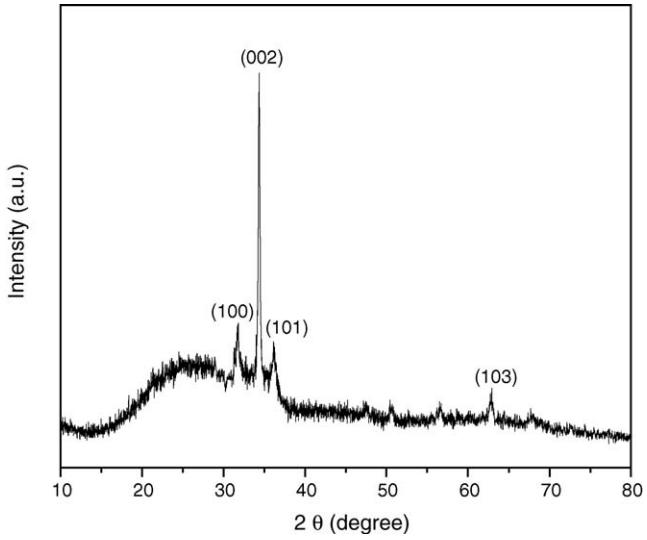

Fig. 3. XRD patterns of ZnO nanorods.

3.2. Crystal structure

According to the XRD patterns of ZnO nanorods (Fig. 3), the diffraction peaks of the obtained ZnO crystals can be indexed to a hexagonal wurtzite structure with cell constants of $a = 0.324$ nm and $c = 0.519$ nm (JCPDS card No. 36-1451). XRD results also indicate strong preferred orientation along the *c*-axis because the [0 0 2] reflection is greatly enhanced relative to the usual [1 0 1] maximum reflection. Further structural characterization of the ZnO crystals was performed by TEM and selected area electron diffraction. We notice from TEM images (Fig. 4(a)) that the average diameter of ZnO nanorods is about 25 nm, and from HRTEM images (Fig. 4(b)) that the spacing between adjacent lattice planes is about 0.26 nm, which corresponds to the

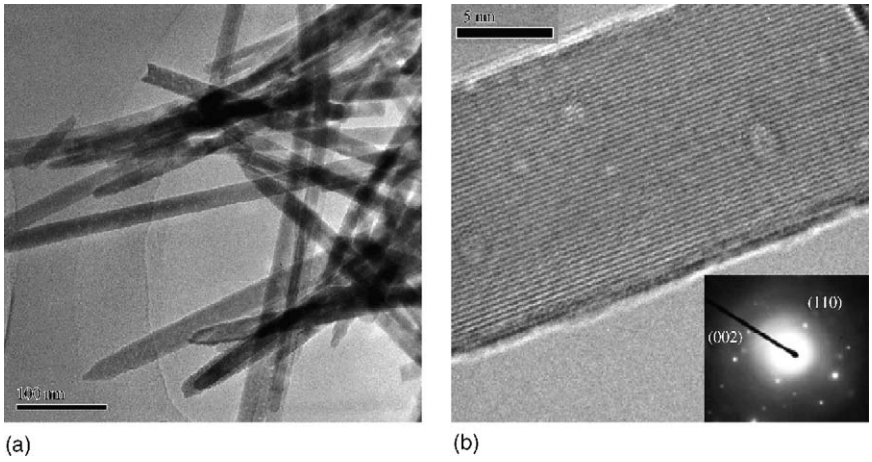

Fig. 4. TEM (a) and HRTEM and SAED (b) of ZnO nanorods.

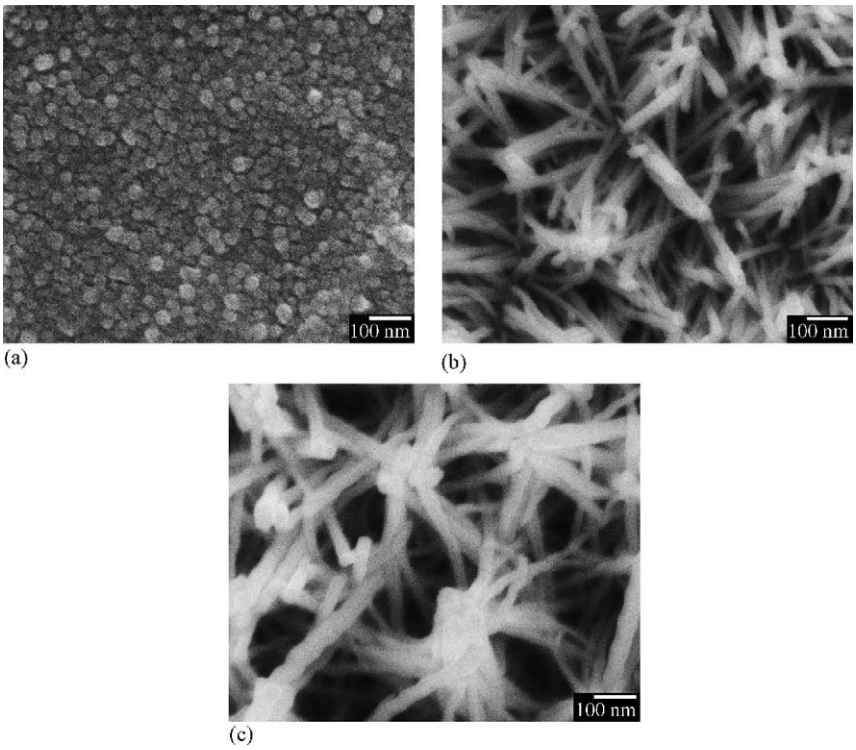

Fig. 5. SEM photographs of the ZnO nanorods grown at different precursor concentration.

distance between two (0 0 2) planes in ZnO crystal.[22] The electron diffraction pattern (Fig. 4(b)) can be assigned to hexagonal ZnO single crystals in the (1 $\bar{1}$ 0) beam direction. Both the high-resolution TEM and SAED results suggest that [0 0 1] is the preferred growth direction for ZnO nanorods.

3.3. Effects of reaction conditions on nanorod morphology

3.3.1. Concentration

For the experiments studying the effect of concentration, the precursor concentration was chosen at 10^{-4} M, 10^{-3} M and 10^{-2} M, and the corresponding concentration of NaOH was 0.025 M, 0.1 M and 1.6 M in the metastable region (Fig. 1) to create the needed degree of supersaturation for rod growth. Fig. 5 shows SEM photographs of the ZnO nanorods grown under 70 °C for 1.5 h. It is found from Fig. 5(a) that only equiareal crystallites can be seen and there is almost no rod growth. Thus it can be concluded that despite the high supersaturation, rods cannot grow well because of the low concentration. Obvious rod growth can be observed in Fig. 5(b) and (c), straight nanorods growing on the whole substrate surfaces with high density and with rod length varying from ~700 nm for 10^{-3} M Zn^{2+} to ~1.5 μm for 10^{-2} M Zn^{2+}. While zinc ion concentration strongly affected the growth rate and rod length, it had a smaller effect on rod diameter, which increases from 25 nm for 10^{-3} M $Zn^{2+}$to 40 nm for 10^{-2} M Zn^{2+}. It should be pointed out that the increasing rate of rod width in our case is not as large as that reported in Vayssieres' work,[23] where the nanorods were prepared on modified substrates and the rod width increased the same order of magnitude as the concentration of reactant. This suggests that, for the ZnO nanorods prepared on modified substrates, the precoated ZnO nanoparticle layer plays the main role in governing the rod diameter; while on the other hand, the rod diameter can also be controlled to some extent by monitoring the concentration of the reactant.

3.3.2. Temperature

The temperature range over which rod growth occurred was 30–90 °C. Fig. 6 exhibits SEM photographs of the ZnO nanorods grown at this temperature range under 10^{-3} M for 1.5 h. We note from Fig. 6(a) that the rods grown at 30 °C are very short and stand perpendicularly to the substrate, indicatng that the growth rate of nanorods is low and the main process taking place might be the formation of hexagonal ZnO crystalline grains. From other pictures, ZnO nanorods are seen to incline to different degree and the average diameter of the nanorods remains almost unchanged; but the average length of the nanorods increases greatly with temperature increasing up to 90 °C. This implies that the growth rate along [0 0 1] direction is more sensitive to temperature compared to those along [1 0 1] and [1 0 0] direction. Fig. 7 shows the film thickness as a function of temperature for 10^{-3} M and 10^{-2} M Zn^{2+} ion solutions. As shown, a maximum growth rate of about 700 nm in 1.5 h for 10^{-3} M Zn^{2+} was achieved at 70 °C. At higher concentrations (e.g. 10^{-2} M Zn^{2+}), however, maximum growth rate was achieved at higher temperatures (e.g. 90 °C for 10^{-2} M Zn^{2+}). In general, such a maximum is evidence of two opposing trends. The growth factors are the increasing rate of ionic diffusion with increasing temperature and the decreasing influence of the activation energy. The opposing factor is the increasing solubility of the

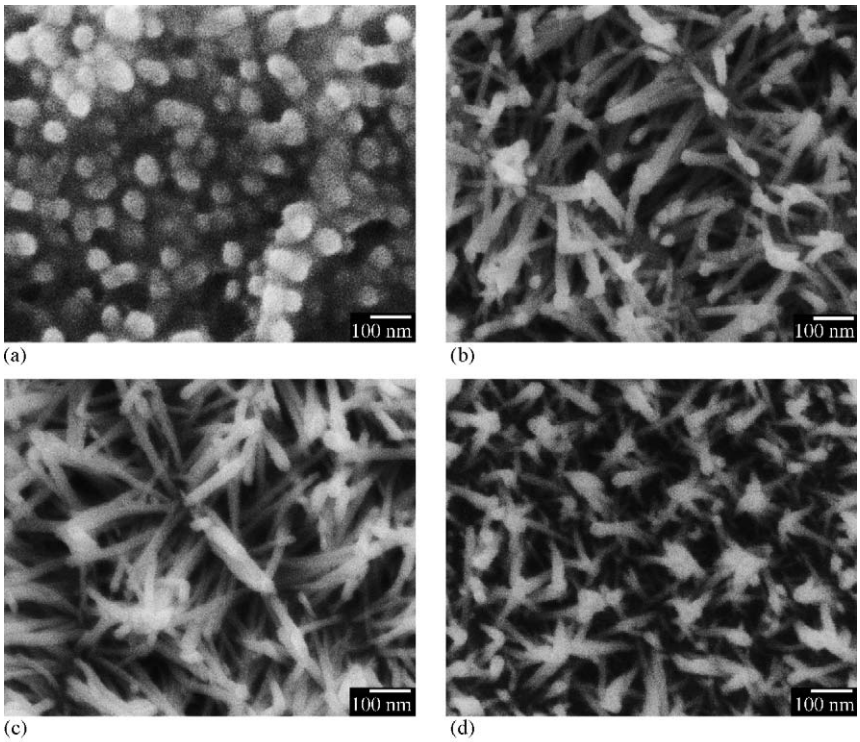

Fig. 6. SEM photographs of the ZnO nanorods grown at different temperatures.

ZnO with temperature. The first factor apparently dominates at lower temperature, while the second dominates at higher temperature, resulting in a peak in the nanorod growth rate versus temperature.

3.3.3. Time

The dependence of the average diameter and film thickness of nanorods on deposition time under 10^{-3} M and 70 °C is illustrated in Fig. 8. Both the growth rates in the radial and axial direction are observed to elevate in the beginning, and then slow with time as the result of decreasing Zn^{2+} concentration. We also found that spiked tips occurred in films grown for less than 4 h (Fig. 4), while flat tips appeared in films grown for 8 h. All the results indicate that the solution had reached equilibrium and the top of rods, viz. the (0 0 2) plane, is dissolved.

3.4. Controlling rod morphology by controlled seed layer with PEG assisting

Fig. 9 shows XRD patterns of ZnO-coated substrates prepared using a sol with added PEG and the resultant nanorods grown under 10^{-3} M and 70 °C for 1.5 h. From Fig. 9(a), it is

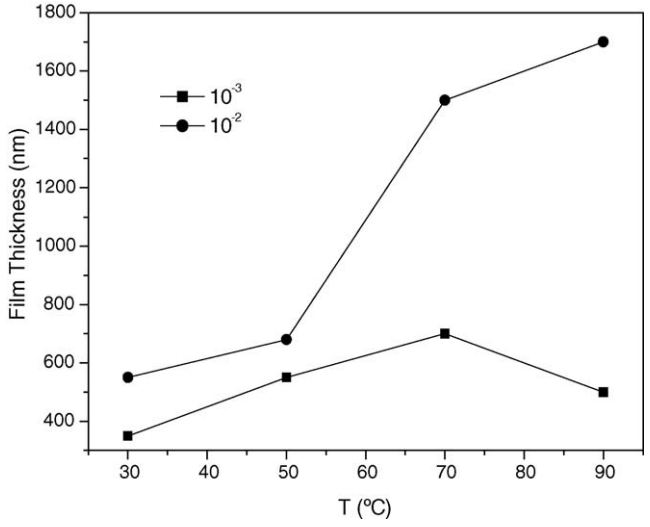

Fig. 7. Film thickness as a function of temperature for 10^{-3} M and 10^{-2} M Zn^{2+} ion solutions.

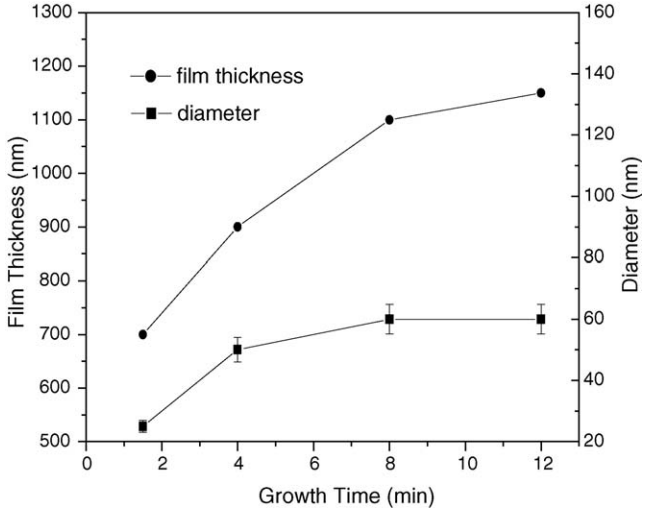

Fig. 8. The dependence of the average diameter and film thickness of nanorods on deposition time.

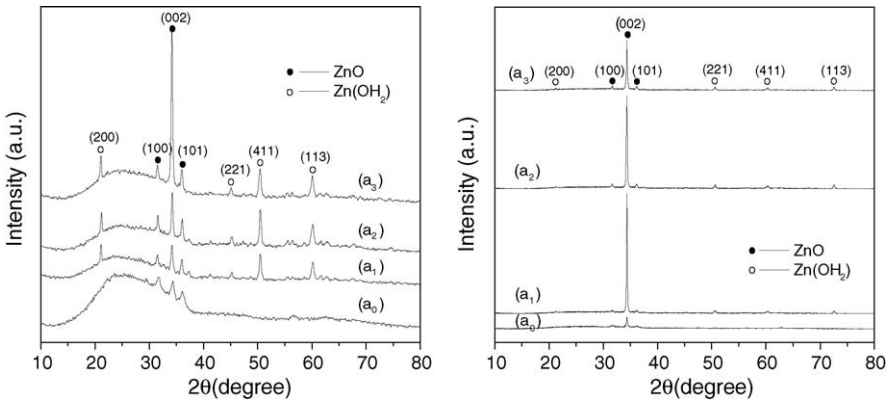

Fig. 9. XRD patterns of ZnO-coated substrates (a) and resultant nanorods (b) prepared by sol added PEG. The amount of PEG: (a_0) and (b_0) 0 g/50 ml; (a_1) and (b_1) 1 g/50 ml; (a_2) and (b_2) 2 g/50 ml; (a_3) and (b_3) 4 g/50 ml.

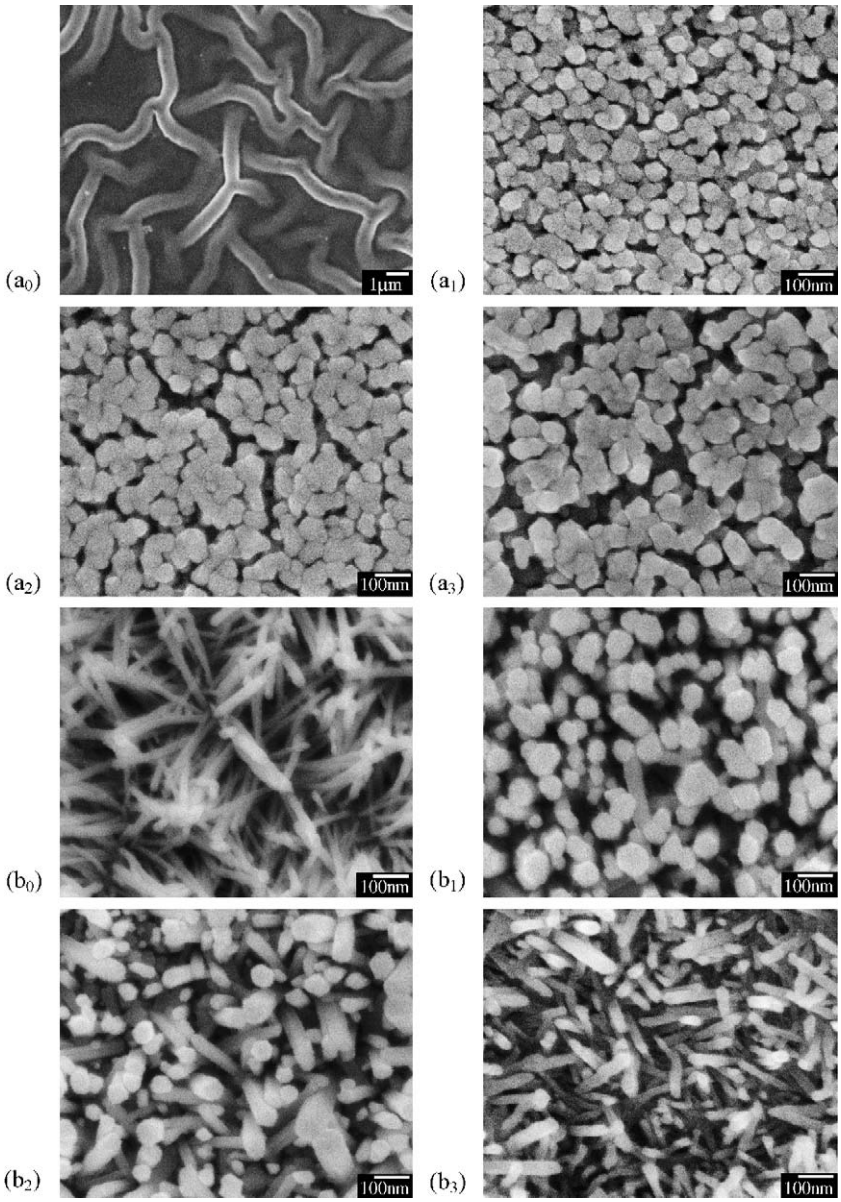

Fig. 10. SEM photographs of ZnO seed surface (a) and the resultant nanorods (b) prepared by sol added PEG. The amount of PEG: (a_0) and (b_0) 0 g/50ml; (a_1) and (b_1) 1 g/50 ml; (a_2) and (b_2) 2 g/50 ml; (a_3) and (b_3) 4 g /50 ml.

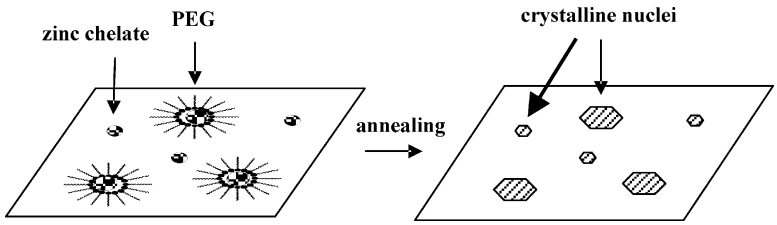

Fig. 11. Schematic diagram of the ZnO nucleation on the PEG-assisted controlled seed surface.

clearly seen that the peak intensity of the (0 0 2) plane of the substrates becomes higher with the increased amount of PEG in the seed sol, showing the increasing degree of orientation along the *c*-axis. From Fig. 9(b), however, the peak intensity of the (0 0 2) plane of the resultant nanorods is found to become higher first and then lower with the increased amount of PEG, and so does the degree of orientation along the *c*-axis of the nanorods.

Fig. 10 exhibits SEM photographs of the ZnO seed surface prepared by sol added PEG and the resultant nanorods grown under 10^{-3} M and 70 °C for 1.5 h. When the amount of PEG is 1 g/50 ml, the seed surface has evenly dense and large crystallites compared to that without PEG, and the growing nanorods have larger diameters and are perpendicularly oriented to the substrate. But with the amount of PEG increasing, the defects in coverage occur and become larger, and the resulting nanorods become thinner and begin to slope.

PEG is usually used as a surfactant to modify the morphology of nanocrystalline films.[24] This phenonenon may be relevant to the template assembly of PEG taking part in texure formation on the seed surface. Fig. 11 suggests a schematic diagram of the ZnO nucleation on the PEG-assisted controlled seed surface. When the proper amount of PEG is added in the seed sol, the hydrophilic terminal hydroxyl groups of PEG adsorb on the zinc acetate oligomer just like the action of PEG adsorbed on titania and zirconia surfaces,[25] while the rather hydrophobic oxyethylene chain exposed to the 2-methoxyethanol, form micelles acting as microreactors, in which the zinc acetate oligomer was enveloped. When substrates were annealed after the dip-coating, PEG was removed at the same time, resulting in highly *c*-oriented large ZnO seeds from the oligomers inside the microreactor. This further induces high density and large size of nuclei, which leads to densely distributed and thick nanorods standing perpendicularly on to the substrates. When more PEG is added, the decomposition and vaporization of PEG become more obvious and leaves defects, which expose the underlying seed layer simultaneously. Regardless of the good orientation along the *c*-axis, the density of nuclei of the underlying layer is low, and their size is small due to the lack of precursor caused by competition of growth between two different seed layers. Under this condition, the rods on the underlying layer have smaller size and slant to some extent. When PEG is further added, larger defects come into being, and the competition of growth between the upper and lower layer leads to lower density and small size of nuclei on both layers, which thus brings about thin rods inclining.

4. Conclusion

A new system deriving from $Zn(NO_3)_2$/NaOH was demonstrated as suitable to prepare ZnO nanorod arrays on ZnO-coated glass sildes. The metastable region between the theoretical thermodynamic equilibrium curve and the measured supersaturation curves for ZnO was used to prepare effectively ZnO nanorods without precipitation of other zinc species. The preparing conditions such as precursor concentration, growth temperature and deposition times have a great influence on the morphology of ZnO nanorods. With the Zn^{2+} ion concentration increasing, the average diameter of ZnO nanorods increases slightly, while the growth rate rises tremendously. The maximum rod growth rate at any given concentration of Zn^{2+} occurs at a specific temperature, and the optimal temperature increases with Zn^{2+} ion concentration. The rate of rod growth gradually lowers with deposition time. Adding of PEG into the seed sol gives a high density and large size of crystallites on the seed surface and obviously changes the morphology of the nanorods, which become densely thick nanorods standing perpendicularly to the substrate.

Acknowledgement

We gratefully acknowledge financial support (Project No. 033802311) from Natural Science Foundation of Tianjin.

References

1. Cui, Y. and Lieber, C. M., Functional nanoscale electronic devices assembled using silicon nanowire building blocks. *Science*, 2001, **291**, 851–853.
2. Emanettoglu, N. W., Gorla, C., Lio, Y., Liang, S. and Lu, Y., Epitaxial ZnO piezoelectric thin films for SAW filters. *Mater. Sci. Semicond. Process.*, 1999, **2**, 247–252.
3. Chen, Y., Bagnall, D. and Yao, T., ZnO as a novel photonic material for the UV region. *Mater. Sci. Eng. B*, 2000, **75**, 190–198.
4. Saito, N., Haneda, H., Sekiguchi, T., Ohashi, N., Sakaguchi, I. and Koumoto, K., Low-temperature fabrication of light-emitting zinc oxide micropatterns using self-assembled monolayers. *Adv. Mater.*, 2002, **14**, 418–420.
5. Liang, S., Sheng, H., Liu, Y., Hio, Z., Lu, Y. and Shen, H., ZnO Schottky ultraviolet photodetectors. *J. Cryst. Growth*, 2001, **225**, 110–113.
6. Lee, J. Y., Choi, Y. S., Kim, J. H., Park, M. O. and Im, S., Optimizing n-ZnO/p-Si heterojunctions for photodiode applications. *Thin Solid Films*, 2002, **403**, 553–557.
7. Koch, M. H., Timbrell, P. Y. and Lamb, R. N., Influence of film crystallinity on the coupling efficiency of ZnO optical modulator waveguides. *Semicond. Sci. Technol.*, 1995, **10**, 1523–1527.
8. Lin, Y., Zhang, Z., Tang, Z., Yuan, F. and Li, J., Characterization of ZnO-based varistors prepared from nanometre precursor powders. *Adv. Mater. Opt. Electron.*, 1999, **9**, 205–209.

9. Golego, N., Studenikin, S. A. and Cocivera, M., Sensor photoresponse of thin-film oxides of zinc and titanium to oxygen gas. *J. Electrochem. Soc.*, 2000, **147**, 1592–1594.
10. Huang, M. H., Mao, S., Feick, H., Yan, H., Wu, Y., Kind, H. *et al.*, Room-temperature ultraviolet nanowire nanolasers. *Science*, 2001, **292**, 1897–1899.
11. Izaki, M. and Ohmi, T., Electrolyte optimization for cathodic growth of zinc oxide films. *J. Electrochem. Soc.*, 1996, **143**, L53–L55.
12. Haga, K., Katahira, F. and Watanabe, H., Preparation of ZnO films by atmospheric pressure chemical-vapor deposition using zinc acetylacetonate and ozone. *Thin Solid Films*, 1999, **343**, 145–147.
13. Ambia, M. G., Islam, M. N. and Hakim, M. O., Effects of deposition variables on the spray pyrolysis of ZnO thin film. *J. Mater. Sci.*, 1994, **29**, 6575–6580.
14. Choi, J. H., Tabata, T. and Kawai, T., Initial preferred growth in zinc oxide thin films on Si and amorphous substrates by a pulsed laser deposition. *J. Cryst. Growth*, 2001, **226**, 493–500.
15. Izaki, M. and Ohmi, T., Transparent zinc oxide films chemically prepared from aqueous solution. *J. Electrochem. Soc.*, 1997, **144**, L3–L5.
16. Izaki, M. and Katayama, J., Characterization of boron-incorporated zinc oxide film chemically prepared from an aqueous solution. *J. Electrochem. Soc.*, 2000, **147**, 210–213.
17. Ito, K. and Nakamura, K., Preparation of ZnO thin films using the flowing liquid film method. *Thin Solid Film*, 1996, **286**, 35–36.
18. Vayssieres, L., Keis, K., Lindquist, S.-E. and Hagfeldt, A., Purpose-build anisotropic metal oxide material: 3D highly oriented micro array of ZnO. *J. Phys. Chem. B*, 2001, **105**, 3350–3352.
19. Vayssieres, L., Keis, K., Lindquist, S.-E. and Hagfeldt, A., Three-dimensional array of highly oriented crystalline ZnO microtubes. *Chem. Mater.*, 2001, **13**, 4395–4398.
20. Peterson, R., Fields, C. and Gregg, B., Epitaxial chemical deposition of ZnO nanocolumns from NaOH solutions. *Langmuir*, 2004, **20**, 5114–5118.
21. Yamabi, S. and Imai, H., Growth conditions for wurtzite zinc oxide films in aqueous solutions. *J. Mater. Chem.*, 2002, **12**, 3773–3778.
22. Schulz, H. and Thiemann, K. H., Structure parameters and polarity of the wurtzite type compounds SiC-2H and ZnO. *Solid State Commun.*, 1979, **32**, 783–785.
23. Vayssieres, L., Growth of arrayed nanorods and nanowires of ZnO from aqueous solutions. *Adv. Mater.*, 2003, **15**, 464–466.
24. Bu, S. J., Jin, Z. G. and Liu, X. X., Preparation and formation mechanism of porpous TiO_2 films using PEG and alcohol solvent as double-templates. *J. Sol–gel. Sci. Technol.*, 2004, **30**, 239–248.
25. Siffert, B. and Li, J. F., Determination of the fraction of bound segments of PEG polymers at the oxide. Water interface by microcalorimetry. *Colloids. Surf.*, 1989, **40**, 207–217.